Contents lists available at ScienceDirect

Chinese Journal of Physics

journal homepage: www.elsevier.com/locate/cjph

Charged anisotropic gravitational decoupled strange stars via complexity factor

S. Sadiq [a,*], Rabia Saleem [b]

[a] Department of Mathematics, Division of Science and Technology, University of Education, Lahore, Pakistan
[b] Department of Mathematics, COMSATS University Islamabad, Lahore Campus, Pakistan

ARTICLE INFO

Keywords:
Exact solutions
Anisotropy
Gravitational decoupling

ABSTRACT

This paper develops a charged anisotropic spherically symmetric strange star model by constructing an exact solution of the field equations through the gravitational decoupling approach. We employ minimal geometric deformation through which the initial decoupled system is divided into Einstein–Maxwell and quasi-Einstein systems. We choose a known solution for isotropic spherical matter distribution with MIT bag equation of state including electromagnetic field and generalize it to an anisotropic model by solving quasi-Einstein field equations using complexity factor. We study the physical viability of the resulting charged anisotropic solution by plotting metric functions, density, pressure, anisotropy parameter, energy conditions, and stability criterion for the strange star candidates SAXJ1808.4-658, SMCX-1, 4U1538-52 as well as HERX-1. It is noticed that all the physical aspects are well-behaved, ensuring the physical acceptability of the developed models.

1. Introduction

Stars are extensively recognized astronomical bodies and are considered as essential building blocks of the galaxy. The burning of atomic fuel happens in the interior of a star to keep its equilibrium state against internal gravitational force. At the point, when the balance state is upset (gravity defeats the pressure), the collapse process happens which is believed to be accountable for the development of neutron stars, white dwarfs, and black holes (compact stellar objects). These bodies carry smaller radii, larger values of densities, and possess strong magnetic effects in contrast with the normal stellar objects. In the center of neutron stars, a phase transition of neutrons to strange quark matter (containing a similar number of up, down, and strange quarks) happens. The up and down quarks are changed into strange matter prompting the development of strange stars.

The interior structure of compact bodies is well-portrayed by determining solutions of the Einstein field equations. The first analytical solution was presented by Schwarzschild [1] depicting a static spherical stellar body which inspired the researchers to inspect the interior construction of these bodies through physically appropriate solutions. Tolman [2] solved the field equations for spherical matter configuration and examined the joining of developed interior models with the exterior solution. Lemaitre [3] analyzed the first anisotropic model by examining the static energy density and radial pressure. Tolman [2] and Oppenheimer [4] demonstrated the compact stellar bodies by considering an ideal Fermi gas equation of state (EoS) and obtained the realistic compact stellar models in close proximity with the observational information.

The authors in [5] considered anisotropic spherical fluid distribution having uniform energy density and deduced that anisotropy can significantly describe high redshift objects like quasars. Heintzmann and Hillebrandt [6] examined anisotropic neutron stars at

* Corresponding author at: Department of Mathematics, Division of Science and Technology, University of Education, Lahore, Pakistan.
E-mail addresses: sobia.sadiq@ue.edu.pk (S. Sadiq), rabiasaleem@cuilahore.edu.pk (R. Saleem).

https://doi.org/10.1016/j.cjph.2022.07.017
Received 19 February 2022; Received in revised form 12 July 2022; Accepted 23 July 2022

higher densities, and showed that there is no constraint on mass for large anisotropy. Herrera and Santos [7] examined anisotropic effects in self-gravitating systems and determined stable models. In [8], Gokhroo and Mehra proposed that stability is enhanced for positive anisotropic factor leading to construction of more compact objects. Dev and Gleiser [9] analyzed the stability of the anisotropic system by considering small radial adiabatic oscillation and explained that compact stellar objects having surface redshift ($Z_s > 2$) can be explained by taking the anisotropic distribution of matter in the interior [10]. Sharma and Maharaj [11] found analytical solutions for anisotropic fluid distribution with linear EoS to describe spherical stellar objects. Sharif and Sadiq [12,13] analyzed the equilibrium configuration of static spherical and cylindrical anisotropic polytropes. Azam and his collaborators [14,15] extended these configurations to generalized polytropic EoS.

The effect of charge in self-gravitating systems is significant in a sense that the stellar models that fail to meet the admissibility criteria are called physically viable. Bonnor [16] investigated some isotropic solutions with the electromagnetic field. Xingxiang [17] studied the physical features of the analytical solution for static spherical charged isotropic matter configuration. Ivanov [18] explored that the inclusion of charge magnifies the stability of the self-gravitating system, and singularities can be prohibited in the process of collapse. Di Prisco et al. [19] analyzed a connection between the Weyl tensor and inhomogeneity of energy density, and discussed the electromagnetic effects on the dynamics of collapsing sphere. Pant and Rajasekhara [20] explored a variety of interior solutions for Einstein–Maxwell field equations and found that the resulting solutions are worthwhile for modeling the super dense stars. Kiess [21] derived an exact Maxwell–Einstein spacetime for static spherically symmetric isotropic matter distribution and found that a range of radius, mass, and charge values can be produced. Sharif and Bhatti [22] illustrated the structure of physical quantities as well as energy constraints for anisotropic spherical solutions under electromagnetic field. Takisa and Maharaj [23] developed analytical solutions of the dynamical equations using polytropic EoS, which yields the modeling of charged anisotropic compact spheres. Khan and his collaborators [24] discussed the electromagnetic effects on anisotropic collapsing sphere along with cosmological constant. They found that the presence of charge improves the rate of destruction.

The non-linear nature of Einstein field equations produces difficulties in determining the analytical solutions. The minimal gravitational decoupling approach [25] is most convenient in finding the analytical as well as physically admissible solutions. Ovalle and Linares [26] used this approach to find the exact solution of the field equations for perfect fluid spherical configuration. Casadio et al. [27] modified temporal and radial metric functions and determined an exterior spherical solution, representing a naked singularity at the Schwarzschild radius. Ovalle [28] constructed anisotropic models from isotropic solutions by gravitational decoupled sources. Ovalle et al. [29] discussed the extension of interior isotropic solution for static stellar models to anisotropic ones. In [30], the authors employed this approach to isotropize the anisotropic model and used complexity factor to generate new solutions. Sharif and collaborators [31–34] formulated some anisotropic solutions for charged/uncharged spherical and cylindrical configurations by decoupling gravitational sources.

Maurya [35] developed charged anisotropic class I solution for the stellar body using complete geometric deformation and demonstrated that this technique is an influential strategy to construct a physically well-behaved solution for the description of compact stellar object. Maurya [36] obtained the physical acceptability of completely deformed embedding class I solution for the compact object possessing charged anisotropic matter distribution. Maurya et al. [37] studied anisotropic compact objects by means of gravitational decoupling using extended geometric deformation and analyzed the feasibility of constructed model through mathematical, physical, and graphical analysis. Tello-Ortiz [38] analyzed spherical imperfect fluid distribution with a dark matter component by interpreting the temporal component of additional source as the dark side of the fluid configuration. They discussed the feasibility of the salient model for some particular strange star candidates. Maurya et al. [39] investigated the stellar interiors for ultra-dense anisotropic spherical systems within the framework of modified gravity and examined the behavior of density, pressure, dynamical equilibrium, energy conditions, and stability. Maurya et al. [40] developed gravitational decoupled anisotropic spherical model within the framework of Rastall theory of gravity and used observational data to examine the limits of the theory under the constructed model.

Maurya et al. [41] presented two classes of solutions for compact objects using complete geometric deformation within the vicinity of Einstein–Gauss–Bonnet theory of gravity. They found that the radial deformation function is non-zero at the boundary of an object for both pressure and density constraints while in the case of minimal geometric deformation, this deformation function vanishes at the boundary for pressure constraint only. Maurya et al. [42] employed Karmarkar condition to examine a complete deformed anisotropic spherically symmetric solution along with electromagnetic effects and found the physical acceptability of the obtained model. Maurya et al. [43] used gravitational decoupling as well as embedding technique to develop self-gravitating structures in modified gravity. They discussed the matching conditions and analyzed the impact of mimic constraint on the mass function. Maurya et al. [44] established an exact anisotropic interior solution in Einstein–Gauss–Bonnet gravity and determined the regularity in interior spacetime. Maurya et al. [45] explored the characteristics of a gravitational decoupled anisotropic model with polytropic EoS within the context of Einstein–Gauss–Bonnet gravity. They concluded that the Einstein–Gauss–Bonnet coupling constant as well as the decoupling parameter plays an influential role in magnifying and conquering the density and radial pressure at interior points of the compact object.

The relativistic models are significant if they exhibit stable structure. Herrera [46] suggested the idea of cracking (when total forces on a system in radial direction shifting from positive to negative) and overturning (when the signs of radial forces reverses from negative to positive) to explore the nature of isotropic/anisotropic matter distribution when the equilibrium is being disturbed. He demonstrated that isotropic fluid configuration stays stable whereas anisotropy leads to the appearance of cracking in a system. Abreu et al. [47] widen the notion of cracking using a speed of sound for spherically symmetric anisotropic matter distribution and deduced that the configuration is not stable for $v_{st}^2 > v_{sr}^2$ (v_{sr}^2 and v_{st}^2 represent radial and tangential speeds of sound, respectively). Sharif and Sadiq [48] explored the stability criterion for anisotropic polytropes under electromagnetic field and configured that compact object endures stable structure for appropriate values of perturbed polytropic parameter. Mardan and Azam [49] considered charged anisotropic cylinder with the polytropic EoS and discussed that the established model is not stable for various values of polytropic parameters.

Our aim is to construct anisotropic strange star models by formulating exact solution of the field equations from a known isotropic solution including an electromagnetic field via minimal gravitational decoupling (MGD) approach. The paper is arranged as follows. Section 2 provides the fundamental formalism of MGD and the Einstein field equations are formulated correspondingly. The junction conditions are utilized to analyze the matching of interior and exterior spacetimes. Section 3 is devoted to obtain an exact anisotropic charged solution with the MIT bag model and examine the physical properties of the derived solution. The results are concluded in the last section.

2. Matter distribution and MGD approach

For a gravitational decoupled system, the action can be illustrated by addition of the Lagrangian density for an additional source as

$$S=\int\left[\frac{R}{16\pi}+L_M+L_E+L_Y\right]\sqrt{-g}d^4x, \tag{1}$$

where $L_M,\ L_E,\ L_Y$ represent the Lagrangian for matter, electromagnetic fields and additional source, respectively, and R is the Ricci scalar. The variation of above action with respect to the metric tensor $g_{\mu\nu}$, we find the field equations for charged decoupled system as

$$G_{\mu\nu}=-8\pi\left(T^{(\mathrm{tot})}_{\mu\nu}+E_{\mu\nu}\right), \tag{2}$$

where

$$T^{(\mathrm{tot})}_{\mu\nu}=T_{\mu\nu}+\varepsilon Y_{\mu\nu}.$$

Here, the additional source $Y_{\mu\nu}$ is coupled to gravitational source via parameter ε. The additional source may generate anisotropies in self-gravitating bodies and contains some other fields (scalar, vector or tensor). The energy–momentum tensors for ideal fluid ($T_{\mu\nu}$) and electromagnetic field ($E_{\mu\nu}$) are defined as

$$\begin{aligned}
T_{\mu\nu} &= (\rho+P)V_\mu V_\nu-Pg_{\mu\nu},\\
E_{\mu\nu} &= \frac{1}{4\pi}\left(-F_\mu{}^{\alpha}F_{\nu\alpha}+\frac{1}{4}F^{\alpha\beta}F_{\alpha\beta}g_{\mu\nu}\right).
\end{aligned}$$

In the above expression, $\rho,\ P,\ V_\mu$ and $F^{\mu\nu}$ stand for density, pressure, four-velocity and the Maxwell field tensor, respectively. The Maxwell field equations are given as

$$F^{\mu\nu}{}_{;\nu}=\mu_0 J^\mu,\quad F_{[\mu\nu;\gamma]}=0,$$

where μ_0 denotes the magnetic permeability and J^μ indicates the four current. In comoving coordinates, the four-velocity and four-current are defined as

$$\phi_\mu=\phi\delta^0_\mu,\quad J_\mu=\zeta V_\mu,$$

here $\zeta=\zeta(r)$ and $\phi=\phi(r)$ represent the charge density and scalar potential, respectively. As an interior geometry, we take the static spherically symmetric line element as

$$ds^2=e^{a(r)}dt^2-e^{b(r)}dr^2-r^2\left(d\theta^2+\sin^2\theta d\phi^2\right). \tag{3}$$

For decoupled system (2), the corresponding field equations are obtained as

$$T^{0(\mathrm{tot})}_0+E^0_0=\frac{e^{-b}}{8\pi}\left(\frac{b'}{r}-\frac{1}{r^2}+\frac{e^b}{r^2}\right), \tag{4}$$

$$T^{1(\mathrm{tot})}_1+E^1_1=\frac{1}{r^2}-\frac{e^{-b}}{8\pi}\left(\frac{a'}{r}+\frac{1}{r^2}-\frac{e^b}{r^2}\right), \tag{5}$$

$$T^{2(\mathrm{tot})}_2+E^2_2=\frac{-e^{-b}}{16\pi}\left(a''+\frac{a'^2}{2}+\frac{a'-b'}{r}-\frac{a'b'}{2}\right), \tag{6}$$

where $T^{0(\mathrm{tot})}_0=T^0_0+\varepsilon Y^0_0$, $T^{1(\mathrm{tot})}_1=T^1_1+\varepsilon Y^1_1$ and $T^{2(\mathrm{tot})}_2=T^2_2+\varepsilon Y^2_2$. The conservation equation ($T^{\mu(\mathrm{tot})}{}_{\nu;\mu}=0$), illustrating the equilibrium stellar structure is turn out to be

$$\begin{aligned}
T^{1'}_1 &+ E^{1'}_1-\frac{a'}{2}\left(T^0_0-T^1_1+E^0_0-E^1_1\right)-\frac{2}{r}\left(T^2_2-T^1_1\right)-\frac{2}{r}\left(E^2_2-E^1_1\right)\\
&-\frac{a'\varepsilon}{2}\left(Y^0_0-Y^1_1\right)+\varepsilon Y^{1'}_1-\frac{2\varepsilon}{r}\left(Y^2_2-Y^1_1\right)=0.
\end{aligned} \tag{7}$$

We find the non-zero components of Maxwell field tensor as

$$F^{01}=\frac{q}{r^2}e^{-\frac{a+b}{2}}=-F^{10},$$

where the electric charge ($q(r)$), and electric field ($E(r)$), can be written as

$$q(r) = 4\pi \int_0^r \zeta r^2 e^{b/2} dr = r^2\sqrt{-F_{10}F_{10}}, \quad E^2(r) = -F_{10}F_{10} = \frac{q^2}{r^4}.$$

The non-vanishing components of $T^{\nu}_{\ \mu}$ and $E^{\nu}_{\ \mu}$ can be expressed as

$$T^0_0 = \rho, \quad T^1_1 = T^2_2 = -P, \quad E^0_0 = E^1_1 = -E^2_2 = \frac{q^2}{8\pi r^4}.$$

Making use of above components, we obtain the following components of $T^{\nu(tot)}_{\mu}$

$$\begin{aligned} T^{0(\text{tot})}_0 &= \rho + \varepsilon Y^0_0 = \rho^{(\text{tot})}, \\ -T^{1(\text{tot})}_1 &= P - \varepsilon Y^1_1 = P^{(\text{tot})}_r, \\ -T^{2(\text{tot})}_2 &= P - \varepsilon Y^2_2 = P^{(\text{tot})}_t. \end{aligned}$$

Also, the hydrostatic equilibrium equation takes the form

$$P' + \frac{a'}{2}(\rho + P) - \frac{EE'}{4\pi} + \frac{a'\varepsilon}{2}\left(Y^0_0 - Y^1_1\right) - \varepsilon Y^{1\prime}_1 - \frac{2\varepsilon}{r}\left(Y^2_2 - Y^1_1\right) = 0. \tag{8}$$

Now, we follow the systematic scheme introduced by Ovalle [25] to obtain solution of the system of Eqs. (4)–(7) containing eight unknown functions ($a, b, \rho, P, q, Y^0_0, Y^1_1, Y^2_2$). We assume an isotropic fluid model (ξ, η, ρ, P, E) for the spacetime given as

$$ds^2 = e^{\xi(r)}dt^2 - \frac{dr^2}{\eta(r)} - r^2\left(d\theta^2 + \sin^2\theta d\phi^2\right),$$

with $\eta = 1 - \frac{2m}{r} + E^2r^2$ with m being the Misner–Sharp mass of fluid distribution. We employ the minimal geometric deformation in metric functions (ξ, η) to integrate the impact of additional source $Y_{\mu\nu}$ in charged isotropic fluid model as [25]

$$\xi \mapsto a = \xi, \quad \eta \mapsto e^{-b} = \eta + \varepsilon f, \tag{9}$$

here f be the deformation function corresponding to radial metric component. The substitution of Eq. (9) in (4)–(6) leads to two systems of the field equations. The first set corresponding to charged perfect fluid configuration ($\varepsilon = 0$) is given as

$$8\pi\rho + E^2 = \frac{1-\eta}{r^2} - \frac{\eta'}{r}, \tag{10}$$

$$8\pi P - E^2 = \frac{\eta - 1}{r^2} + \frac{\eta\xi'}{r}, \tag{11}$$

$$8\pi P + E^2 = \frac{\eta\xi''}{2} + \frac{\eta\xi'^2}{4} + \frac{\eta\xi'}{2r} + \frac{\xi'\eta'}{4} + \frac{\eta'}{2r}, \tag{12}$$

and the conservation equation is

$$P' + \frac{a'}{2}(\rho + P) - \frac{EE'}{4\pi} = 0. \tag{13}$$

The solution of Eqs. (10)–(12) describes the internal structure of stellar body for charged isotropic matter distribution. For this case, the radial metric function is given as

$$\eta = 1 - \frac{2m}{r} + r^2E^2 = 1 - \frac{8\pi}{r}\int_0^r \left(\rho + \frac{r^2E^2}{8\pi}\right) r^2 dr + r^2E^2.$$

The second system corresponding to the additional source represents the quasi-Einstein system given as

$$8\pi Y^0_0 = -\left(\frac{f'}{r} + \frac{f}{r^2}\right), \tag{14}$$

$$8\pi Y^1_1 = -f\left(\frac{a'}{r} + \frac{1}{r^2}\right), \tag{15}$$

$$8\pi Y^2_2 = -\frac{f}{2}\left(a'' + \frac{a'^2}{2} + \frac{a'}{r}\right) - \frac{f'}{2}\left(\frac{a'}{2} + \frac{1}{r}\right), \tag{16}$$

$$Y^{1\prime}_1 = -\frac{a'}{2}\left(Y^1_1 - Y^0_0\right) + \frac{2}{r}\left(Y^2_2 - Y^1_1\right). \tag{17}$$

We observe that the inclusion of an additional source makes the isotropic matter distribution to be anisotropic. The smooth joining of interior ($r < R$) and exterior ($r > R$) regions is provided by the matching conditions that play fundamental part in examining the progression of relativistic bodies. For the present case, the interior spacetime representing stellar object is given as

$$ds^2_- = e^{a_-}dt^2 - \left(1 - \frac{2\tilde{m}}{r} + r^2E^2\right)^{-1} dr^2 - r^2\left(d\theta^2 + \sin^2\theta d\phi^2\right), \tag{18}$$

here $\tilde{m}$ is the internal mass for $T^{(\text{tot})}_{\mu\nu}$. In the absence of $Y_{\mu\nu}$, we have vacuum solution for the outer geometry while the inclusion of additional source may introduce some new fields and hence the exterior is no more vacuum. As an outer geometry, we consider the general outer metric as

$$ds_+^2 = e^{a_+}dt^2 - e^{b_+}dr^2 - r^2\left(d\theta^2 + \sin^2\theta d\phi^2\right). \tag{19}$$

The first fundamental form ($[ds^2]_\Sigma = 0$, Σ represents the hypersurface) of junction conditions yields

$$a_-(R) = a_+(R), \quad 1 - \frac{2M_0}{R} + E_0^2R^2 + \varepsilon f(R) = e^{-b_+(R)}, \tag{20}$$

where $M_0 = m(R)$ and $E_0 = E(R)$ shows total mass and electric intensity inside the sphere, respectively while $f(R)$ is radial geometric deformation at surface of a star. The second fundamental form ($[T^{(\text{tot})}_{\mu\nu}S^\nu]_\Sigma = 0$, S^ν denotes the radial unit four-vector) provides

$$P(R) - \frac{E_0^2}{8\pi} - \varepsilon(Y_1^1(R))_- = -\varepsilon(Y_1^1(R))_+. \tag{21}$$

Making use of Eq. (15) in the above equation, we get

$$P(R) - \frac{E_0^2}{8\pi} - \frac{\varepsilon f}{8\pi}\left(\frac{1}{R^2} + \frac{a'}{R^2}\right) = -\varepsilon(Y_1^1(R))_+, \tag{22}$$

which yields

$$P(R) - \frac{E_0^2}{8\pi} + \frac{\varepsilon f}{8\pi}\left(\frac{1}{R^2} + \frac{a'}{R^2}\right) = \frac{\varepsilon g}{8\pi}\left(\frac{2}{R^2}\frac{(\frac{\mathcal{M}}{R} - \mathbb{E}^2R^2)}{1 - \frac{2\mathcal{M}}{R} + \mathbb{E}^2R^2} + \frac{1}{R^2}\right), \tag{23}$$

where g represents the deformation function undergone by the exterior Reissner–Nordström metric due to extra source $Y_{\mu\nu}$ as

$$ds_+^2 = \left(1 - \frac{2\mathcal{M}}{R} + \mathbb{E}^2R^2\right)dt^2 - \left(1 - \frac{2\mathcal{M}}{R} + \mathbb{E}^2R^2\right)^{-1}dr^2 - r^2\left(d\theta^2 + \sin^2\theta d\phi^2\right).$$

The necessary and sufficient conditions for smooth joining of the interior MGD spacetime with spherically symmetric outer metric explained by deformed Reissner–Nordström (RN) line-element (consists of the fields generated by source $Y_{\mu\nu}$) are shown by Eqs. (20) and (23). If the outer metric is assumed to be the standard RN metric, then Eq. (23) becomes

$$\overline{P}(R) \equiv P(R) - \frac{E_0^2}{8\pi} + \frac{\varepsilon f}{8\pi}\left(\frac{1}{R^2} + \frac{a'}{R^2}\right) = 0. \tag{24}$$

It is well-known that a star stays in its equilibrium state when the effective pressure vanishes at surface. If positive geometric deformation in interior metric exists and weakens the gravitational field, an exterior RN vacuum can only be compatible with a non-vanishing inner $Y_{\mu\nu}$ if the ideal stellar matter has $P(R) < 0$ at the surface of the star. Nevertheless, the condition $P(R) = 0$ can be determined by imposing that the right side of Eq. (24) must be proportional to $P(R) - \frac{E_0^2}{8\pi}$, i.e., $P(R) - \frac{E_0^2}{8\pi} \sim \varepsilon(Y_1^1)_-$ in Eq. (21) which provides the disappearance of inner deformation $f(R)$.

In the next section, we consider a known isotropic spherical model for strange star with charge to complete our systematic analysis.

3. Gravitational decoupled anisotropic solution

To consider a known solution for the corresponding field equations is a key point in deriving the anisotropic solutions using MGD approach. We observe that two systems of Eqs. (5)–(8) and (14)–(16) consist of six non-linear equations in eight unknowns. The strange quark matter is well-described by a simple EoS known as MIT Bag model according to which the quarks are massless as well as non-interacting. This model is very helpful in the study of balance state of an ultra-dense compact objects [50–54] represented as

$$P = \frac{1}{3}(\rho - 4B).$$

Deb et al. [55] found stable static spherically symmetric anisotropic singularity free solution for strange stars by considering this model. They found that the increase in anisotropy of compact stars occurs with the radius and possesses its maximum value at the boundary. Maurya and Tello-Ortiz [56] developed charged anisotropic exact solution for compact stars satisfying MIT bag model and concluded that anisotropic force initially predominates the Coulomb force while the electric force predominates the anisotropic one with the increase in radius. Jasim et al. [57] investigated static spherically symmetric isotropic strange stars via MIT bag model and deduced that the proposed model is viable. We consider charged strange star model [57] given as

$$e^a = e^\xi = Kr^{2n}, \tag{25}$$

$$\begin{aligned}\eta^{-1} &= \left\{\left(3+2n+n^2\right)\left(1+n+n^2\right)r^{\frac{2+2n+2n^2}{2+n}}\right\}\left\{r^{\frac{2+2n+2n^2}{2+n}}\left(3 - 16Br^2\pi\right.\right.\\ &+ n^2\left(1-16B\pi r^2\right) + n\left(2-16B\pi r^2\right)\Big) - 2M\left(1+n+n^2\right)(3+2n\\ &+ n^2)\,R + n(1+n)\left(3+2n+n^2\right)R^2 + 16B\left(1+n+n^2\right)\pi R^4 + E_0^2\\ &\times R^4\left(n^2+n+1\right)\left(n^2+2n+3\right)R^{\frac{2n^2-2}{n+2}}\Bigg\}^{-1},\end{aligned} \tag{26}$$

$$\begin{aligned}
\rho &= \left[\varrho\left(n+\frac{1}{2}\right)r^{\frac{-2n^2-2n-2}{n+2}}+16(n+2)\left\{B\pi r^2n^4+\frac{3n^3}{16}+n^2\left(6B\pi r^2\right.\right.\right.\\
&+\left.\left.\left.\frac{3}{8}\right)+\left(5B\pi r^2+\frac{9}{16}\right)n+6B\pi r^2\right\}\right]\left\{\left(\left(n^2+2n+3\right)\left(n^2+n+1\right)\right.\right.\\
&\times\left.\left.16(n+2)\pi r^2\right)\right\}^{-1}, \qquad (27)\\
P &= \left[\varrho\left(n+\frac{1}{2}\right)r^{\frac{-2n^2-2n-2}{n+2}}-48(n+2)\left\{B\pi r^2n^4+\left(4B\pi r^2-\frac{1}{16}\right)n^3\right.\right.\\
&+\left.\left.n^2\left(6B\pi r^2-\frac{1}{8}\right)+\left(5B\pi r^2-\frac{3}{16}\right)n+2B\pi r^2\right\}\right]\left\{\left(n^2+2n+3\right)\right.\\
&\times\left.482\pi r^2\left(n^2+n+1\right)(n+2)\right\}^{-1}, \qquad (28)\\
q^2 &= r^4\left[-\varrho(n+3)r^{\frac{-2n^2-2n-2}{n+2}}-48n(n+1)(n+2)\left\{\left(B\pi r^2-\frac{1}{8}\right)n^3-3\right.\right.\\
&\times\left.\left.\frac{n^2}{16}-\frac{n}{4}-B\pi r^2+\frac{3}{16}\right\}\right]\left\{\left(6(n+2)\left(n^2+n+1\right)\left(n^2+2n+3\right)\right.\right.\\
&\times\left.\left.(n+1)r^2\right)\right\}^{-1}, \qquad (29)
\end{aligned}$$

where

$$\begin{aligned}
\varrho &= 96\left(n+\frac{1}{2}\right)(n+1)\left[\frac{n}{16}\left(n^2+2n+3\right)(n+1)R^{\frac{2(n^2+n+1)}{n+2}}+\left\{R^{\frac{2n^2+4n+6}{n+2}}\right.\right.\\
&\times\left.\left.B\pi+\frac{1}{8}\left(\frac{R^{\frac{2(n^2-1)}{n+2}}E_0^2R^4}{2}-R^{\frac{2n^2+n}{n+2}}M\right)\left(n^2+2n+3\right)\right\}\left(n^2+n+1\right)\right]. \qquad (30)
\end{aligned}$$

Here, K and n are arbitrary constants while B is the bag constant. For the standard RN spacetime as an outer geometry, the first and second fundamental forms of junction conditions yield

$$\begin{aligned}
E_0^2 &= \frac{16B\pi R^3n+16B\pi R^3+4Mn^2-2Rn^2+6Mn-3Rn+2M}{(2n^2+3n+1)R^3}, \qquad (31)\\
K &= \left\{1-\frac{2M}{R}+E_0^2R^2\right\}\left(\frac{1}{R}\right)^{2n}, \qquad (32)\\
n &= \frac{1}{8(4B\pi R^3-3)}\left[112B\pi R^3+6M-9R+\left(18688B^2\pi^2R^6-3264BM\pi\right.\right.\\
&\times\left.\left.R^3-2016B\pi R^4+36M^2-108MR+81R^2\right)^{\frac{1}{2}}\right]. \qquad (33)
\end{aligned}$$

In order to find the anisotropic model, we incorporate the effects of ε in the inner region. Eqs. (25) and (9) represent the temporal and radial metric coefficients, respectively, while f and $Y_{\mu\nu}$ are related to Eqs. (14)–(16) whose solution will be obtained by considering an extra constraint, which is a complexity factor [58–61]. Herrera [62] added a quite different definition of complexity for a self-gravitating body. This definition is associated with the perception of spherical structure but is not associated with disequilibrium/information. He used the concept of Tolman mass, which is dependent on the energy density inhomogeneity as well as the anisotropic pressure that represents a single scalar function dubbed as complexity factor. It vanishes when these two terms cancel each other or in the presence of isotropic pressure as well as energy density homogeneity. The orthogonal splitting of Riemann tensor yields a scalar that represents a complexity factor. The complexity factor for charged static spherically symmetric gravitational decoupled system is a scalar function $Y_{TF}^{(\mathrm{tot})}$, defined as

$$\begin{aligned}
Y_{TF}^{(\mathrm{tot})} &= \left(\frac{5}{2}-8\pi\right)\frac{q^2}{r^4}-\frac{4\pi}{r^3}\int_0^r\tilde{r}\rho'^{(\mathrm{tot})}d\tilde{r}+8\pi\Pi^{(\mathrm{tot})},\\
&= \left(\frac{5}{2}-8\pi\right)\frac{q^2}{r^4}-\frac{4\pi}{r^3}\int_0^r\tilde{r}\rho'd\tilde{r}+8\pi\Pi-\frac{4\pi\varepsilon}{r^3}\int_0^r\tilde{r}Y_0^{0'}d\tilde{r}+8\pi\Pi_Y,\\
&= Y_{TF}+Y_{TF}^{Y}, \qquad (34)
\end{aligned}$$

where Y_{TF} is the complexity factor for charged perfect fluid system while the complexity factor Y_{TF}^{Y} appears due to the presence of additional source. Andrade and Contreras [63] used generalization of the complexity factor obtained from the Tolman IV solution to extend the Wyman IIa, Tolman IV, Heintzmann IIa and Durgapal IV solutions to the anisotropic ones. Arias et al. [64] constructed anisotropic models for self-gravitating objects fulfilling the vanishing complexity condition and obtained the feasible as well as stable solution for particular choice of parameters. Maurya et al. [65] employed this condition as well as the gravitational decoupling approach to construct anisotropic solution for embedding class I spacetime and examined the physical viability of the resulting solution. Maurya et al. [66] investigated the role of gravitational decoupling on isotropization of the anisotropic spherical solution using complete geometric deformation as well as the complexity factor. They discussed the impact of decoupling constant as well as the compactness parameter on the complexity factor.

We consider that charged isotropic fluid configuration as well as an additional source has the same complexity factor, i.e., Y_{TF} associated with $T_{\mu\nu}+E_{\mu\nu}$ remains the same after inclusion of $\Upsilon_{\mu\nu}$, implying $Y_{TF}^{\Upsilon}=0$. This condition can be written as

$$\Pi_{\Upsilon}=\varepsilon\left(\Upsilon_1^1-\Upsilon_2^2\right)=\frac{4\pi\varepsilon}{r^3}\int_0^r \tilde{r}\Upsilon_0^{0\prime}d\tilde{r}. \tag{35}$$

Using Eqs. (14)–(17) in the above equation, we find a first order ordinary differential equation as

$$f'\left(\xi'+\frac{4}{r}\right)+f\left(2\xi''+\xi^2-\frac{2\xi'}{r}-\frac{8}{r^2}\right)=0.$$

Making use of Eq. (25), we obtain following solution of the above equation

$$f(r)=(2r+nr)^{\frac{4+4n-2n^2}{2+n}}C_1, \tag{36}$$

where C_1 is an integration constant. Substituting the above geometric deformation function in Eqs. (9) and (14)–(17), we find

$$\begin{aligned} e^{-b} &= \frac{r^{\frac{-2\left(1+n+n^2\right)}{2+n}}}{\left(3+2n+n^2\right)\left(1+n+n^2\right)}\left\{r^{\frac{2\left(1+n+n^2\right)}{2+n}}\left(3-16B\pi r^2+(1-16B\pi\right.\right.\\ &\times\left. r^2\right)n^2+n\left(2-16B\pi r^2\right))-2M\left(3+2n+n^2\right)\left(1+n+n^2\right)R+n\\ &\times (1+n)\left(3+2n+n^2\right)R^2+16B\left(1+n+n^2\right)\pi R^4+\left(1+n+n^2\right)\\ &\times \left. Q^2R^{\frac{2\left(n^2-1\right)}{2+n}}\left(3+2n+n^2\right)\right\}+C_1\left\{(2+n)r\right\}^{\frac{4+4n-2n^2}{2+n}}\varepsilon, \end{aligned} \tag{37}$$

$$\begin{aligned} \rho^{(\text{tot})} &= \left[\left(3n^3+96B\pi r^2+16Bn^4\pi r^2+n\left(9+80B\pi r^2\right)+n^2\left(6+96B\pi r^2\right)\right)\right.\\ &\times \left.(2+n)+96\left(\frac{1}{2}+n\right)^2(1+n)r^{-\frac{2\left(1+n+n^2\right)}{2+n}}\varpi_1\right]\left[\left(16\left(1+n+n^2\right)\pi r^2\right.\right.\\ &\times \left.\left.(2+n)\left(3+2n+n^2\right)\right)+\frac{C_1\left(2n^2-5n-6\right)\left((2+n)r\right)^{\frac{2+3n-2n^2}{2+n}}\varepsilon}{8\pi r}\right]^{-1}, \end{aligned} \tag{38}$$

$$\begin{aligned} P_r^{(\text{tot})} &= \varpi_1\varpi_2\left[\left(48(2+n)\left(1+n+n^2\right)\left(3+2n+n^2\right)\pi r^2\right)+\frac{C_1(1+2n)\varepsilon}{8\pi r^2}\right.\\ &\times \left.\left((2+n)r\right)^{\frac{4+4n-2n^2}{2+n}}\right]^{-1}, \end{aligned} \tag{39}$$

$$\begin{aligned} P_t^{(\text{tot})} &= \varpi_1\varpi_2\left[\left(48(2+n)\left(1+n+n^2\right)\left(3+2n+n^2\right)\pi r^2\right)-\frac{\left(nr-2n^2+r\right)}{16\pi r^2}\right.\\ &\times \left.\varepsilon\left((2+n)r\right)^{\frac{4+4n-2n^2}{2+n}}C_1\right]^{-1}, \end{aligned} \tag{40}$$

$$\Pi^{(\text{tot})} = -\frac{C_1\left\{(2+n)r\right\}^{\frac{4+4n-2n^2}{2+n}}\left\{2-2n^2+r+n(4+r)\right\}\varepsilon}{16\pi r^2}, \tag{41}$$

where

$$\begin{aligned} \varpi_1 &= \frac{n}{16}(1+n)\left(3+2n+n^2\right)R^{\frac{2\left(1+n+n^2\right)}{2+n}}+\frac{1}{16}\left(1+n+n^2\right)R^{\frac{2\left(n^2-1\right)}{2+n}}\left(Q^2\right.\\ &\times \left.\left(3+2n+n^2\right)+2R\left(8B\pi R^3-M\left(3+2n+n^2\right)\right)\right), \end{aligned} \tag{42}$$

$$\begin{aligned} \varpi_2 &= 3n(2+n)\left(\left(1-64B\pi r^2\right)n^5-32B\pi r^2-16Bn^4\pi r^2-\left(80B\pi r^2-3\right)\right)\\ &+ 96(1+n)\left(\frac{1}{2}+n\right)^2r^{-\frac{2\left(1+n+n^2\right)}{2+n}}. \end{aligned} \tag{43}$$

This solution (25), (37)–(40) represents the minimally deformed (by the generic anisotropic source $\Upsilon_{\mu\nu}$) strange star model. It is worth mentioning here that $\varepsilon\rightarrow 0$ provides the standard perfect fluid charged strange star solution (25)–(29). The second fundamental form of matching conditions described in Eq. (24) provides

$$\begin{aligned} C_1 &= \frac{8\pi R^3((2+n)R)^{\frac{2n^2-4-4n}{2+n}}}{(2n+R)\varepsilon}\left(\left\{3\varpi_1(2+n)\left(n^5\left(64B\pi R^2-1\right)+32B\pi R^2\right.\right.\right.\\ &+ \left.16\pi R^2Bn^4-n\left(3-80B\pi R^2\right)\right)-\left(\frac{1}{2}+n\right)^2(1+n)R^{-\frac{2\left(1+n+n^2\right)}{2+n}}\\ &\times 96\}\left\{\left(48\left(1+n+n^2\right)(2+n)\left(3+2n+n^2\right)\pi R^2\right)\right\}^{-1}+\left\{(3(2+n)\right. \end{aligned}$$

Table 1
Physical parameters for strange stars with $B = 90$ MeV/fm^3.

Strange stars	M ($M_\odot$)	R (km)	Q (columb)	$\frac{M}{R}$	n
SMCX-1	1.04 $\pm$ 0.09	7.321 $\pm$ 0.029	1.333 $\times$ 10^{20}	0.21	0.42
SAXJ1808.4-658	0.9 $\pm$ 0.3	7.235 $\pm$ 0.280	1.676 $\times$ 10^{20}	0.185	0.38
4U1538-52	0.87 $\pm$ 0.07	7.207 $\pm$ 0.072	1.725 $\times$ 10^{20}	0.18	0.37
HERX-1	0.85 $\pm$ 0.15	7.185 $\pm$ 0.169	1.752 $\times$ 10^{20}	0.175	0.36

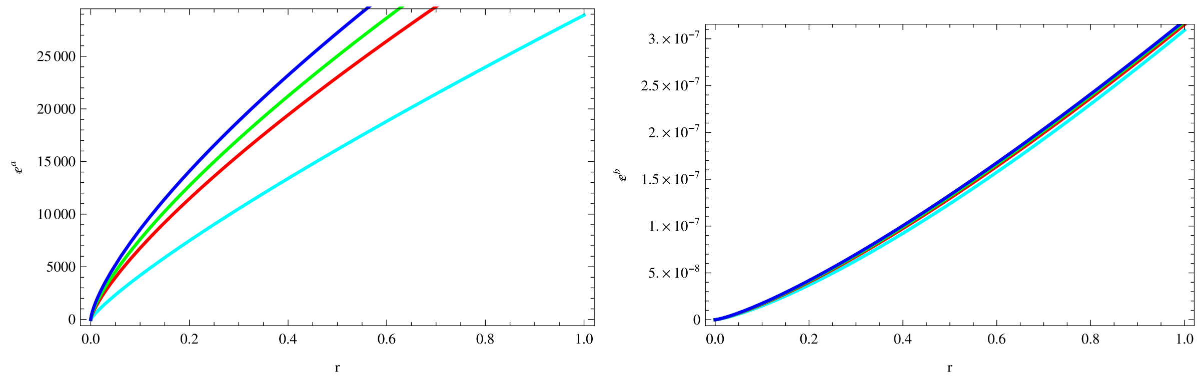

Fig. 1. Plots of temporal (left) and radial (right) metric functions for SMCX − 1 (cyan), SAXJ1808.4 − 658 (red), 4U1538 − 52 (green), HERX − 1 (blue) versus r with $\varepsilon = 0.1$. (For interpretation of the references to color in this figure legend, the reader is referred to the web version of this article.)

$$\begin{aligned}
&\times\ n(1+n)\left(3n^2+4n-3+16B\pi R^2-2n^3\left(8B\pi R^2-1\right)\right)-(1+n)\\
&\times\ 96\left(n+\frac{1}{2}\right)(3+n)R^{-\frac{2\left(1+n+n^2\right)}{2+n}}\varpi_1\Bigg)\Bigg\}\left\{\left(48(1+n)\left(1+n+n^2\right)\right.\right.\\
&\times\ \left.\left.(2+n)\left(3+2n+n^2\right)\pi R^2\right)\right\}^{-1}\Bigg),
\end{aligned}\tag{44}$$

while the continuity of metric potentials yields

$$\begin{aligned}
K \;=\; &\frac{1}{R^{2n}}\left(\frac{R^{-\frac{2\left(1+n+n^2\right)}{2+n}}}{\left(1+n+n^2\right)\left(3+2n+n^2\right)}\left(n(1+n)\left(3+2n+n^2\right)R^2-2M\right.\right.\\
&\times\ \left(1+n+n^2\right)\left(3+2n+n^2\right)R+16B\left(1+n+n^2\right)\pi R^4+\left(1+n+n^2\right)\\
&\times\ \left(3+2n+n^2\right)Q^2R^{\frac{2\left(n^2-1\right)}{2+n}}+R^{\frac{2\left(1+n+n^2\right)}{2+n}}\left(3+n^2\left(1-16B\pi R^2\right)-16\pi\right.\\
&\times\ \left.\left.\left.BR^2+n\left(2-16B\pi R^2\right)\right)\right)+C_1((2+n)R)^{\frac{4+4n-2n^2}{2+n}}\varepsilon\right).
\end{aligned}\tag{45}$$

At present, we examine the physical features of created anisotropic strange star solution through the graphical construction of metric potentials, radial/tangential pressures, energy density, anisotropy parameter, mass function, redshift parameter, compactness, energy constraints and stability. For this purpose, we consider the masses as well as radii of some particular strange star candidates (SMCX − 1, SAXJ1808.4 − 658, 4U1538 − 52, HERX − 1 whose physical parameters are presented in Table 1) and fix the parameters C_1 from Eq. (44) and K from Eq. (45) whereas n will be taken as obtained for the charged perfect fluid case (Eq. (33)). The metric functions ought to be non-singular and regular all through the interior of a star. It is seen that the both metric potentials $e^{a(r)}$ and $e^{b(r)}$ exhibit increasing behavior against radial coordinate r as shown in Fig. 1. The plots of energy density, radial/tangential pressures and anisotropy parameter are plotted in Fig. 2. The stellar bodies demand that these quantities like energy density and radial/tangential pressure must be finite, positive and maximum within the interior of strange stars. It is observed that the density possesses maximum value at the center and decreases monotonically with the increase in r. Additionally, we find that radial and tangential pressures are positive in the interior of a star whereas there is a monotonic decrease with the increase in radial coordinate. The graph of anisotropic factor $\Pi^{(\mathrm{tot})}$ shows that it is positive and finite throughout the stellar constitution. For the physical acceptability of the stellar constitutions, charged anisotropic strange star model should satisfy the energy constraints, i.e., null energy constraint, weak energy constraint, strong energy constraint and dominant energy constraint at each point in the interior of system. For our developed model, these conditions turn out to be

$$\begin{aligned}
&\rho^{(\mathrm{tot})}+\frac{q^2}{8\pi r^4}\geq 0,\quad \rho^{(\mathrm{tot})}+P_r^{(\mathrm{tot})}\geq 0,\quad \rho^{(\mathrm{tot})}-P_r^{(\mathrm{tot})}+\frac{q^2}{4\pi r^4}\geq 0,\\
&\rho^{(\mathrm{tot})}\pm P_t^{(\mathrm{tot})}\geq 0,\quad \rho^{(\mathrm{tot})}+P_r^{(\mathrm{tot})}+2P_t^{(\mathrm{tot})}+\frac{q^2}{4\pi r^4}\geq 0.
\end{aligned}$$

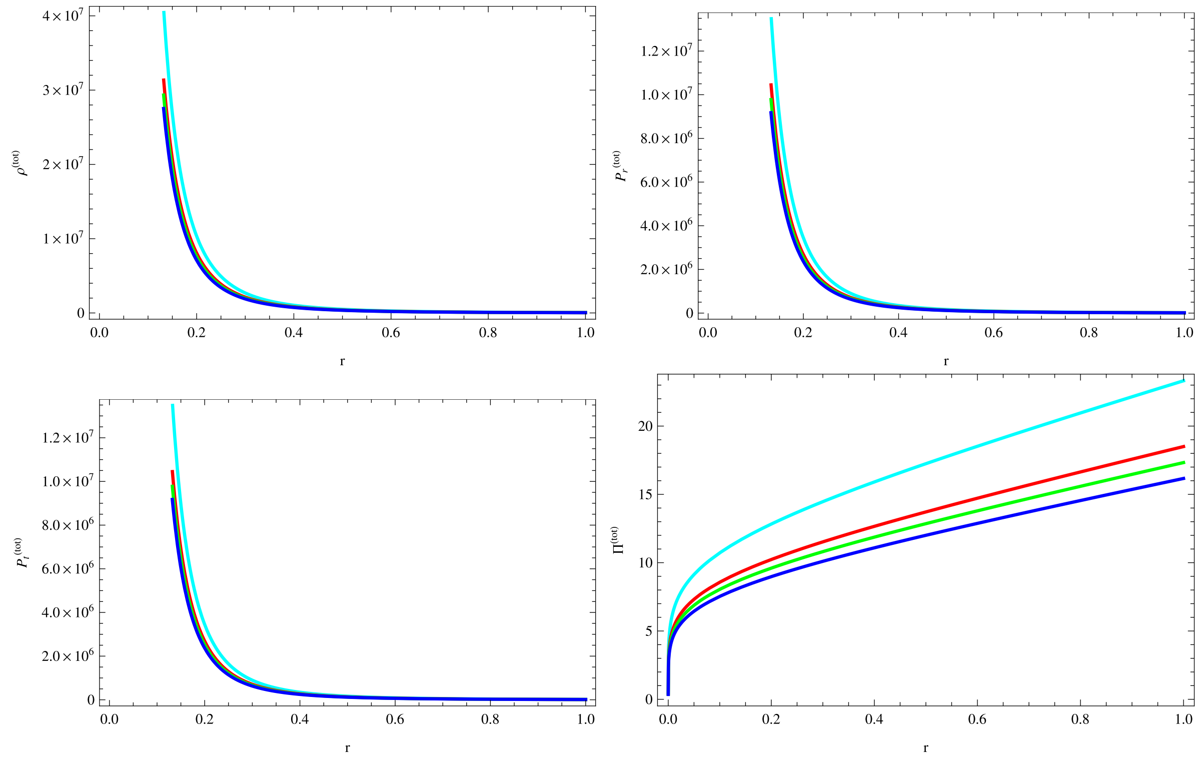

Fig. 2. Plots of density (left plot, upper row), radial pressure (right plot, upper row), tangential pressure (left plot, lower row) and anisotropy (right plot, lower row) for $SMCX-1$ (cyan), $SAXJ1808.4-658$ (red), $4U1538-52$ (green), $HERX-1$ (blue) versus r with $\epsilon = 0.1$. (For interpretation of the references to color in this figure legend, the reader is referred to the web version of this article.)

We present the energy conditions for considered strange star candidates in Fig. 3, which demonstrates that all the energy conditions are satisfied by our charged anisotropic solution for the particular choice of parameters. We analyze the stability of created model by means of sound speed criterion. The radial (v_r^2) as well as tangential (v_t^2) squared speed of sound are determined by the following formulae

$$v_r^2 = \frac{dP_r^{(tot)}}{d\rho^{(tot)}}, \quad v_t^2 = \frac{dP_t^{(tot)}}{d\rho^{(tot)}}. \tag{46}$$

As indicated by the causality condition, the speed of sound ought to be smaller than the speed of light whenever it moves through the anisotropic matter configuration in compact stellar objects. According to this condition, the inequalities $0 \le v_r^2$ and $v_t^2 < 1$ must be fulfilled. The plots of Fig. 4 show that our models fulfill this condition. As indicated by Abreu et al. [47], the region of potentially stable matter configuration is $-1 \le (v_t^2 - v_r^2) \le 0$ whereas $0 \le (v_t^2 - v_r^2) \le 1$ gives potentially unstable region. In the current work, our models fulfill the inequality $-1 \le (v_t^2 - v_r^2) \le 0$ (Fig. 5). Thus, our proposed model is potentially stable.

For a specific density, the adiabatic index demonstrates the stiffness of the EoS. We examine dynamical stability of the celestial structures against radial adiabatic perturbation through adiabatic index. For a matter content becoming anisotropic, the spherical symmetric system is changed only in radial direction to prevent gravitational collapse showing that the radial direction is significant. The Newtonian spheres are stable when the adiabatic index is larger than $4/3$ and if this index is equal to $4/3$, it depicts the neutral equilibrium presented by Bondi [67]. For anisotropic relativistic spherical configuration, this condition turns out to be different and makes the spheres more unstable due to regenerative pressure represented as [68]

$$\Gamma < \frac{4}{3} + \left[\frac{1}{3}\kappa\frac{\rho_0 P_{r0}}{|P'_{r0}|} + \frac{4}{3}\frac{P_{t0} - P_{r0}}{|P'_{r0}|r}\right]_{max},$$

where ρ_0, P_{r0}, P_{t0} indicate the initial density, radial/tangential pressures of the fluid. In the above expression, the second and third terms on right side represent the relativistic and anisotropic corrections. Heintzmann and Hillebrandt [69] demonstrated that the increase of anisotropy in the system changes the stability criterion as $\Gamma > \frac{4}{3}$. Generally, the presence of anisotropy in relativistic spherical configurations have the effect on the stability of stellar bodies. To overcome these instabilities, Moustakidis [70] proposed a critical value of the adiabatic index as

$$\Gamma_{crit} < \frac{4}{3} + \frac{19}{21}u,$$

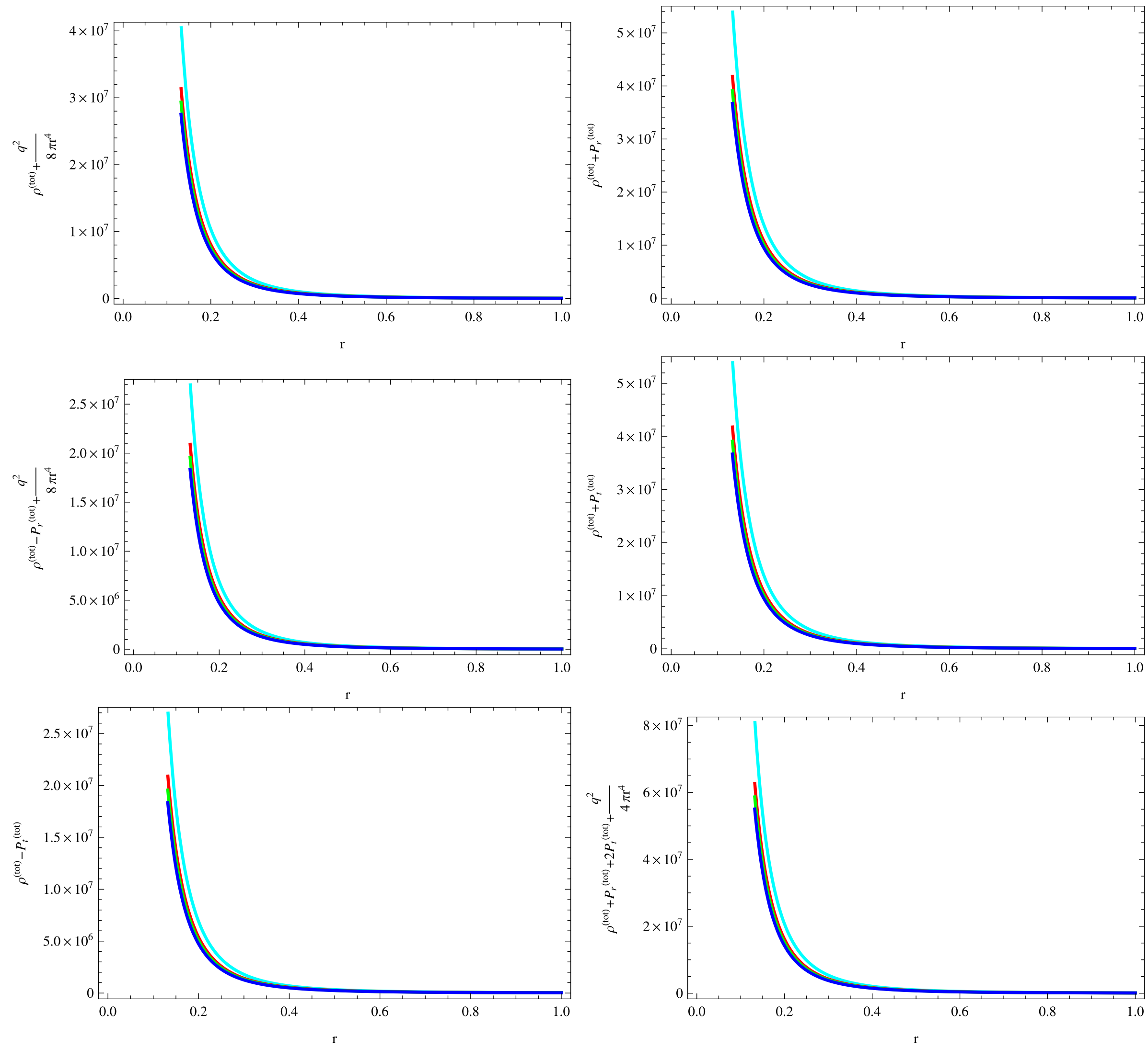

Fig. 3. Plots of energy conditions for SMCX−1 (cyan), SAXJ1808.4−658 (red), 4U1538−52 (green), HERX−1 (blue) versus r and with $\varepsilon = 0.1$. (For interpretation of the references to color in this figure legend, the reader is referred to the web version of this article.)

with u indicating the compactness factor. For the stable matter configuration, it is mandatory that $\Gamma \geq \Gamma_{\text{crit}}$. The radial ($\Gamma_r$) adiabatic index is defined as [71]

$$\Gamma_r^{(\text{tot})} = \left(\frac{\rho^{(\text{tot})} + P_r^{(\text{tot})}}{P_r^{(\text{tot})}}\right)\frac{dP_r^{(\text{tot})}}{d\rho^{(\text{tot})}}. \tag{47}$$

We plot the radial adiabatic indices in Fig. 6, showing that $\Gamma_r^{(\text{tot})} > 4/3$ and monotonically increasing as we move towards the boundary. To discuss the surface redshift of stellar structure, the mass–radius ratio is a key ingredient. Andreasson [72] and Bohmer and Harko [73] proposed this ratio for charged matter distributions as

$$\frac{Q^2(18R^2+Q^2)}{2R^2(12R^2+Q^2)} \leq \frac{M}{R} \leq \frac{2}{9} + \frac{3Q^2+2R\sqrt{R^2+3Q^2}}{9R^2}.$$

We evaluate the lower as well as upper bound of mass–radius ratio and find that the above inequality is satisfied. In terms of this ratio, the redshift function is defined as

$$Z = \left(1 - \frac{2M_0}{R} + \varepsilon f\right)^{-\frac{1}{2}} - 1.$$

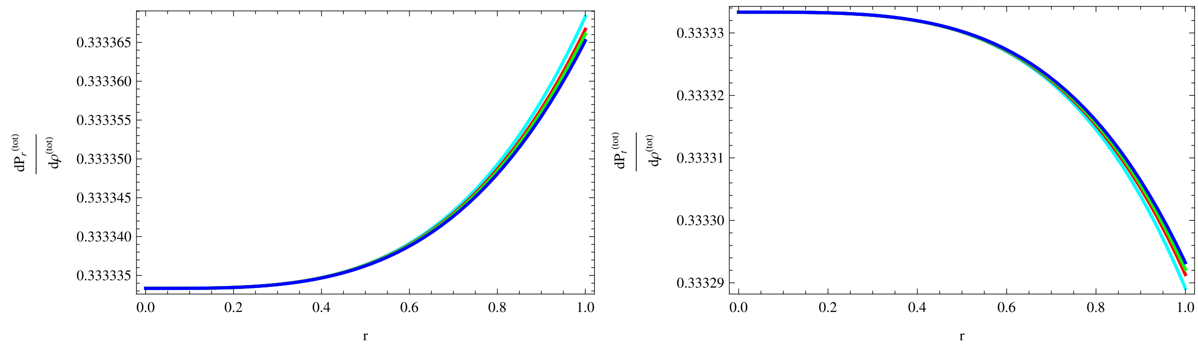

Fig. 4. Plots of radial (left) and tangential (right) sound speeds for SMCX − 1 (cyan), SAXJ1808.4 − 658 (red), 4U1538 − 52 (green), HERX − 1 (blue) versus r and with $\epsilon = 0.1$. (For interpretation of the references to color in this figure legend, the reader is referred to the web version of this article.)

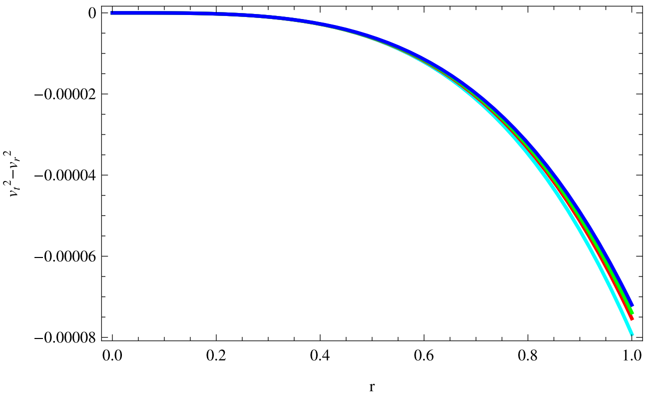

Fig. 5. Plot of $v_t^2 - v_r^2$ for SMCX − 1 (cyan), SAXJ1808.4 − 658 (red), 4U1538 − 52 (green), HERX − 1 (blue) versus r and with $\epsilon = 0.1$. (For interpretation of the references to color in this figure legend, the reader is referred to the web version of this article.)

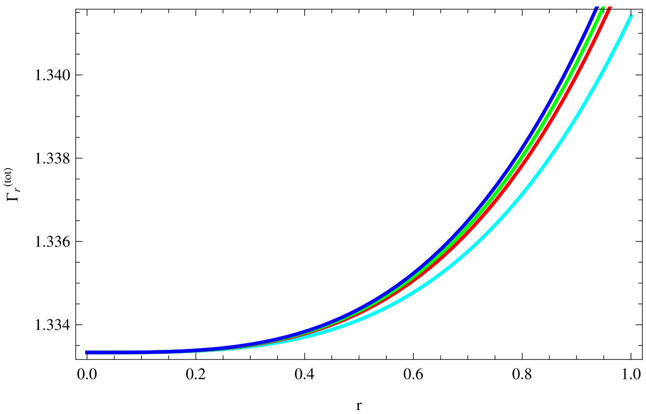

Fig. 6. Plot of radial adiabatic index for SMCX − 1 (cyan), SAXJ1808.4 − 658 (red), 4U1538 − 52 (green), HERX − 1 (blue) versus r and with $\epsilon = 0.1$. (For interpretation of the references to color in this figure legend, the reader is referred to the web version of this article.)

We plot this function for considered strange star candidates in Fig. 7, which shows that the surface redshift attains maximum values in the stellar interior and decreases with the increase in radius.

4. Final remarks

The configuration of stellar interiors is elegantly described by the analytical as well as numerical solutions of the Einstein field equations. In this respect, several authors have solved the field equations using various techniques and discussed their physical

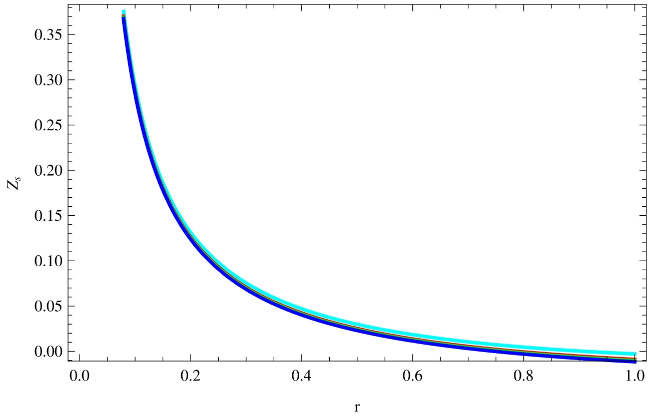

Fig. 7. Plot of surface redshift for SMCX − 1 (cyan), SAXJ1808.4 − 658 (red), 4U1538 − 52 (green), HERX − 1 (blue) versus r and with $\varepsilon = 0.1$. (For interpretation of the references to color in this figure legend, the reader is referred to the web version of this article.)

significance [74–77]. In the study of stellar interiors, the notion of gravitational decoupling by means of the minimal geometric deformation as well as the complete geometric deformation is very significant as it works perfectly to convert the isotropic solutions into anisotropic domain or can be used to obtain new solutions. In the present study, we have employed the MGD technique to formulate a new anisotropic strange star model with charge using a known isotropic solution. According to MGD approach, an additional source is adjoined with the charged perfect fluid stress–energy tensor, which provides the effective field equations. A minimal geometric deformation is introduced in the radial metric function of the spacetime (used for the isotropic case) yielding two sets of the Einstein equations: the first set corresponds to the field equations for perfect fluid along with charge whereas the second set is associated with the new source as well as the deformed metric function. We have compared our interior spacetime with the deformed RN metric and evaluated the junction conditions. To solve quasi-Einstein equations, we have taken the known charged perfect fluid model and then integrated the impact of new source $\Upsilon_{\mu\nu}$. In addition, we have imposed an additional condition to close the system of differential equations, i.e., the charged isotropic system and the decoupled source have the same complexity factors. The consideration of complexity factor for a specific scenario can act as an EoS which may lead close approximation to Einstein field equations. Also, it can act as an additional constraint to reduce the complications in solving the field equations [78,79]. We have considered the masses and radii of four strange star candidates SMCX − 1, SAXJ1808.4 − 658, 4U1538 − 52 and, HERX − 1, and used the junction conditions to determine unknown constants appeared in the constructed solutions. For physical suitability of the derived outcomes, we have investigated the nature of some physical parameters, energy conditions and stability criterion. The results can be summarized as follows

- **Metric Functions:** The metric functions $e^{a(r)}$ and $e^{b(r)}$ exhibit the finite as well as positive graphical structure as we travel towards the boundary of a star and henceforth these are regular as well as appropriate to develop the model for anisotropic matter distribution.
- **Energy Density and Pressures:** It is found that the energy density as well as the radial/ tangential pressures are well-behaved (they are not negative and finite) all through the matter distribution. Likewise the radial/tangential pressures monotonically decrease and disappear at surface of the stars.
- **Anisotropy Parameter:** At the center ($r = 0$), fluid distribution shows isotropic structure whereas the increment in anisotropic factor occurs as one travels towards the surface of a star. In addition, $\Pi^{(\mathrm{tot})} > 0$ intending the existence of repulsive nature of gravitational force which may help in the development of more compact bodies.
- **Energy Conditions:** The graphical structure of all energy conditions indicate that these are satisfied yielding the physical acceptability of the generated solution.
- **Stability Analysis:** The stability criterion is investigated with the aid of adiabatic index criterion and the cracking method. It is seen that these conditions are fulfilled and henceforth the developed solution is stable.

We summarize that our constructed model is significant as it shows physically viable behavior to depict the anisotropic strange stars. Also, our results are consistent with that obtained for the charged isotropic case [57].

Declaration of competing interest

The authors declare that they have no known competing financial interests or personal relationships that could have appeared to influence the work reported in this paper.

References

[1] K. Schwarzschild, On the gravitational field of a mass point according to Einstein's theory, Sitz. Deut. Akad. Wiss. Berlin Kl. Math. Phys. 1916 (1916) 189–196.
[2] R.C. Tolman, Static solutions of Einstein's field equations for spheres of fluid, Phys. Rev. 55 (1939) 364–373.
[3] G. Lemaître, L'univers en expansion, Ann. Soc. Sci. Brux. A 53 (1933) 51–85.
[4] J.R. Oppenheimer, G.M. Volkof, On massive neutron cores, Phys. Rev. 55 (1939) 374–381.
[5] R.L. Bowers, E.P.T. Liang, Anisotropic spheres in general relativity, Astrophys. J. 188 (1974) 657–665.
[6] H. Heintzmann, W. Hillebrandt, Neutron stars with an anisotropic equation of state-mass, redshift and stability, Astron. Astrophys. 38 (1975) 51–55.
[7] L. Herrera, N.O. Santos, Local anisotropy in self-gravitating systems, Phys. Rep. 286 (1997) 53–130.
[8] M.K. Gokhroo, A.L. Mehra, Anisotropic spheres with variable energy density in general relativity, Gen. Relativity Gravitation 26 (1994) 75–84.
[9] K. Dev, M. Gleiser, Anisotropic stars II: stability, Gen. Relativity Gravitation 35 (2003) 1435–1460.
[10] M. Gleiser, K. Dev, Anistropic stars: Exact solutions and stability, Internat. J. Modern Phys. D 13 (2004) 1389–1397.
[11] R. Sharma, S.D. Maharaj, A class of relativistic stars with a linear equation of state, Mon. Not. R. Astron. Soc. 375 (2007) 1265–1268.
[12] M. Sharif, S. Sadiq, Effects of charge on anisotropic conformally flat polytropes, Can. J. Phys. 93 (2015) 1420–1426.
[13] M. Sharif, S. Sadiq, Conformally flat polytropes for anisotropic cylindrical geometry, Can. J. Phys. 93 (2015) 1583–1587.
[14] M. Azam, S.A. Mardan, I. Noureen, M.A. Rehman, Study of polytropes with generalized polytropic equation of state, Eur. Phys. J. C 76 (2016) 1–9.
[15] M. Azam, S.A. Mardan, I. Noureen, M.A. Rehman, Charged cylindrical polytropes with generalized polytropic equation of state, Eur. Phys. J. C 76 (2016) 510–518.
[16] W.B. Bonnor, The equilibrium of a charged sphere, Mon. Not. R. Astron. Soc. 129 (1965) 443–446.
[17] W. Xingxiang, Exact solution of a static charged sphere in general relativity, Gen. Relativity Gravitation 19 (1987) 729–737.
[18] B.V. Ivanov, Maximum bounds on the surface redshift of anisotropic stars, Phys. Rev. D 65 (2002) 104011-104016.
[19] A. Di Prisco, L. Herrera, G. Le Denmat, M.A.H. MacCallum, N.O. Santos, Nonadiabatic charged spherical gravitational collapse, Phys. Rev. D 76 (2007) 064017-064039.
[20] N. Pant, S. Rajasekhara, Variety of well behaved parametric classes of relativistic charged fluid spheres in general relativity, Astrophys. Space Sci. 333 (2011) 161–168.
[21] T.E. Kiess, Exact physical Maxwell-Einstein Tolman-VII solution and its use in stellar models, Astrophys. Space Sci. 339 (2012) 329–338.
[22] M. Sharif, M.Z. Bhatti, Effects of electromagnetic field on shearfree spherical collapse, Astrophys. Space Sci. 347 (2013) 337–348.
[23] P.M. Takisa, S.D. Maharaj, Some charged polytropic models, Gen. Relativity Gravitation 45 (2013) 1951–1969.
[24] S. Khan, H. Shah, Z. Ahmad, M. Ramzan, Final fate of charged anisotropic fluid collapse, Modern Phys. Lett. A 32 (2017) 1750192–1750203.
[25] J. Ovalle, Searching exact solutions for compact stars in braneworld: a conjecture, Modern Phys. Lett. A 23 (2008) 3247–3263.
[26] J. Ovalle, F. Linares, Tolman IV solution in the randall-sundrum braneworld, Phys. Rev. D 88 (2013) 104026-104042.
[27] R. Casadio, J. Ovalle, R. da Rocha, The minimal geometric deformation approach extended, Classical Quantum Gravity 32 (2015) 215020-215030.
[28] J. Ovalle, Decoupling gravitational sources in general relativity: from perfect to anisotropic fluids, Phys. Rev. D 95 (2017) 104019-104023.
[29] J. Ovalle, R. Casadio, R. da Rocha, A. Sotomayor, Anisotropic solutions by gravitational decoupling, Eur. Phys. J. C 78 (2018) 122–139.
[30] R. Casadio, E. Contreras, J. Ovalle, A. Sotomayor, Z. Stuchlik, Isotropization and change of complexity by gravitational decoupling, Eur. Phys. J. C 79 (2019) 826–833.
[31] M. Sharif, S. Sadiq, Gravitational decoupled charged anisotropic spherical solutions, Eur. Phys. J. C 78 (2018) 410–419.
[32] M. Sharif, S. Sadiq, Gravitational decoupled anisotropic solutions for cylindrical geometry, Eur. Phys. J. Plus 133 (2018) 245–255.
[33] M. Sharif, Q. Ama-Tul-Mughani, Gravitational decoupled solutions of axial string cosmology, Modern Phys. Lett. A 35 (2020) 2050091–2050104.
[34] M. Sharif, S. Ahmed, Gravitationally decoupled non-static anisotropic spherical solutions, Modern Phys. Lett. A 36 (2021) 2150145–2150160.
[35] S.K. Maurya, A completely deformed anisotropic class one solution for charged compact star: a gravitational decoupling approach, Eur. Phys. J. C 79 (2019) 958–972.
[36] K.N. Singh, S.K. Maurya, M.K. Jasim, F. Rahaman, Minimally deformed anisotropic model of class one space–time by gravitational decoupling, Eur. Phys. J. C 79 (2019) 851–865.
[37] S.K. Maurya, F. Tello-Ortiz, M.K. Jasim, An EGD model in the background of embedding class I space–time, Eur. Phys. J. C 80 (2020) 918–934.
[38] F. Tello-Ortiz, Non-singular solution for anisotropic model by gravitational decoupling in the framework of complete geometric deformation (CGD), Eur. Phys. J. C 80 (2020) 448–459.
[39] S.K. Maurya, A. Errehymy, K.N. Singh, F. Tello-Ortiz, M. Daoud, Gravitational decoupling minimal geometric deformation model in modified $f(R,T)$ gravity theory, Phys. Dark Univ. 30 (2020) 100640-100654.
[40] S.K. Maurya, F. Tello-Ortiz, Decoupling gravitational sources by MGD approach in Rastall gravity, Phys. Dark Univ. 29 (2020) 100577-100595.
[41] S.K. Maurya, F. Tello-Ortiz, M. Govender, Exploring physical properties of gravitationally decoupled anisotropic solution in 5D Einstein-Gauss–Bonnet gravity, Fortschr. Phys. 69 (2021) 2100099–2100113.
[42] S.K. Maurya, A.S. Al Kindi, M.R. Al Hatmi, R. Nag, Complete deformed charged anisotropic spherical solution satisfying Karmarkar condition, Res. Phys. 29 (2021) 104674-104684.
[43] S.K. Maurya, F. Tello-Ortiz, S. Ray, Decoupling gravitational sources in $f(R,T)$ gravity under class I spacetime, Phys. Dark Univ. 31 (2021) 100753-100766.
[44] S.K. Maurya, A. Pradhan, F. Tello-Ortiz, A. Banerjee, R. Nag, Minimally deformed anisotropic stars by gravitational decoupling in Einstein-Gauss–Bonnet gravity, Eur. Phys. J. C 81 (2021) 848–866.
[45] S.K. Maurya, M. Govender, K.N. Singh, N. Riju, Gravitationally decoupled anisotropic solution using polytropic EoS in the framework of 5D Einstein-Gauss–Bonnet gravity, Eur. Phys. J. C 82 (2022) 4961–4973.
[46] L. Herrera, Cracking of self-gravitating compact objects, Phys. Lett. A 165 (1992) 206–210.
[47] H. Abreu, H. Hernández, L.A. Núũez, Cracking of self-gravitating compact objects with local and non local equations of state, J. Phys.: Conf. Ser. 66 (2006) 012038-012046.
[48] M. Sharif, S. Sadiq, Electromagnetic effects on cracking of anisotropic polytropes, Eur. Phys. J. C 76 (2016) 568–575.
[49] S.A. Mardan, M. Azam, Cracking of charged polytropes with generalized polytropic equation of state, Eur. Phys. J C. 77 (2017) 385–397.
[50] A. Sedrakian, The physics of dense hadronic matter and compact stars, Prog. Part. Nucl. Phys. 58 (2007) 168–246.
[51] B. Golf, J. Hellmers, F. Weber, Impact of strange quark matter nuggets on pycnonuclear reaction rates in the crusts of neutron stars, Phys. Rev. C 80 (2009) 015804-015815.
[52] M. Brilenkov, M. Eingorn, L. Jenkovszky, A. Zhuk, Dark matter and dark energy from quark bag model, J. Cosmol. Astropart. Phys. 08 (2013) 002–015.
[53] N.R. Panda, K.K. Mohanta, P.K. Sahu, Radial modes of oscillations of slowly rotating magnetized compact hybrid stars, J. Phys: Conf. Ser. 599 (2015) 012036-012041.
[54] P. Bhar, A new hybrid star model in krori-barua spacetime, Astrophys. Space Sci. 357 (2015) 46–55.
[55] D. Deb, S.R. Chowdhury, S. Ray, F. Rahaman, B.K. Guha, Relativistic model for anisotropic strange stars, Ann. Physics 387 (2017) 239–252.
[56] S.K. Maurya, F. Tello-Ortiz, Generalized relativistic anisotropic compact star models by gravitational decoupling, Eur. Phys. J. C 79 (2019) 33–46.

[57] M.K. Jasim, S.K. Maurya, S. Ray, D. Shee, D. Deb, F. Rahaman, Charged strange stellar model describing by tolman v metric, Res. Phys. 20 (2021) 103648-103657.
[58] J. Sanudo, A.F. Pacheco, Complexity and white-dwarf structure, Phys. Lett. A 373 (2009) 807–810.
[59] K. Chatzisavvas, V.P. Psonis, C.P. Panos, C. Moustakidis, Complexity and neutron star structure, Phys. Lett. A 373 (2009) 3901–3909.
[60] M.G.B. de Avellar, J.E. Horvath, Entropy, complexity and disequilibrium in compact stars, Phys. Lett. A 376 (2012) 1085–1089.
[61] M.G.B. de Avellar, R.A. de Souza, J.E. Horvath, D.M. Paret, Information theoretical methods as discerning quantifiers of the equations of state of neutron stars, Phys. Lett. A 378 (2014) 3481–3487.
[62] L. Herrera, New definition of complexity for self-gravitating fluid distributions: The spherically symmetric, static case, Phys. Rev. D 97 (2018) 044010-044019.
[63] J. Andrade, E. Contreras, Stellar models with like-tolman IV complexity factor, Eur. Phys. J. C 81 (2021) 889–900.
[64] C. Arias, E. Contreras, E. Fuenmayor, A. Ramos, Anisotropic star models in the context of vanishing complexity, Ann. Physics 436 (2022) 168671-168687.
[65] S.K. Maurya, M. Govender, S. Kaur, R. Nag, Isotropization of embedding class I spacetime and anisotropic system generated by complexity factor in the framework of gravitational decoupling, Eur. Phys. J. C 82 (2022) 100–110.
[66] S.K. Maurya, R. Nag, Role of gravitational decoupling on isotropization and complexity of self-gravitating system under complete geometric deformation approach, Eur. Phys. J. C 82 (2022) 48–61.
[67] H. Bondi, The contraction of gravitating spheres, Proc. R. Soc. Lond. Ser. A Math. Phys. Eng. Sci. 281 (1987) 39–48.
[68] S.K. Maurya, R. Nag, MGD solution under class I generator, Eur. Phys. J. Plus 136 (2021) 679–712.
[69] H. Heintzmann, W. Hillebrandt, Neutron stars with an anisotropic equation of state-mass, redshift and stability, Astron. Astrophys. 38 (1975) 51–55.
[70] C. Moustakidis, The stability of relativistic stars and the role of the adiabatic index, Gen. Relativity Gravitation 49 (2017) 88–108.
[71] P. Fuloria, N. Pant, Physical plausibility of cold star models satisfying karmarkar conditions, Eur Phys. J. A 53 (2017) 227–235.
[72] H. Andreasson, Sharp bounds on $2m/r$ of general spherically symmetric static objects, J. Differ. Equ. 245 (2008) 2243–2266.
[73] C.G. Bohmer, T. Harko, Minimum mass–radius ratio for charged gravitational objects, Gen. Relativity Gravitation 39 (2007) 757–775.
[74] Y.K. Gupta, S.K. Maurya, A class of charged analogues of durgapal and fuloria superdense star, Astrophys. Space Sci. 331 (2011) 135–144.
[75] S.K. Maurya, Y.K. Gupta, S. Ray, B. Dayanandan, Anisotropic models for compact stars, Eur. Phys. J. C 75 (2015) 225–235.
[76] S.K. Maurya, A. Banerjee, S. Hansraj, Role of pressure anisotropy on relativistic compact stars, Phys. Rev. D 97 (2018) 044022-044032.
[77] S.K. Maurya, A. Banerjee, M.K. Jasim, J. Kumar, A.K. Prasad, A. Pradhan, Anisotropic compact stars in the Buchdahl model: A comprehensive study, Phys. Rev. D 99 (2019) 044029-044035.
[78] S.K. Maurya, R. Nag, Role of gravitational decoupling on isotropization and complexity of self-gravitating system under complete geometric deformation approach, Eur. Phys. J. C 82 (2022) 1–14.
[79] M. Carrasco-Hidalgo, E. Contreras, Ultracompact stars with polynomial complexity by gravitational decoupling, Eur. Phys. J. C 81 (2021) 757–763.